

# LABORATORY EXAMINATION AND SEASONAL ANALYSIS OF FROSTING AND DEFROSTING FOR AN AIR-TO-AIR HEAT PUMP

W.A. Miller, P.E.  
ASHRAE Associate Member

## ABSTRACT

An air-to-air split-system residential heat pump of nominal 2 3/4-ton (9.7-kW) capacity was instrumented and tested in the laboratory. The coefficient of performance, system capacity, and component efficiencies were measured during steady-state and frosting-defrosting conditions in the heating mode (1) to gain better understanding of the physical processes that affect the performance of the test heat pump and (2) to quantify the frosting and defrosting losses. Cumulative frosting and defrosting loss coefficients were calculated, from which empirical frosting and defrosting algorithms were developed for modeling of frosting and defrosting losses. Seasonal analyses indicate that the test heat pump with tube-and-wavy-fin outdoor coil had 1% to 5% energy loss due to frosting and demand defrosting accounted for only an additional 1% to 3% yearly energy loss. Demand defrost control can reduce yearly frosting-defrosting losses by 5% to 10% over 90- and 45-minute time-temperature controls.

## INTRODUCTION

The frosting and reverse-cycle defrosting of the outdoor heat exchanger of an air-to-air heat pump results in dynamic losses that degrade the efficiency of the heat pump. The frosting of the outdoor heat exchanger necessitates defrosting to ensure system reliability and efficiency. During the defrosting operation, the heat pump runs in the cooling mode, which requires use of auxiliary heaters to temper the chilled supply air. Both reverse-cycle operation and use of resistance heat during defrost cause degradation of coefficient of performance (COP) and capacity.

Previous work has been done on a split-system heat pump having a spine-fin outdoor heat exchanger (Miller 1982, 1983). This series of laboratory experiments was conducted on a split-system 2 3/4-ton (9.7-kW) air-to-air heat pump having tube-and-plate-fin heat exchangers. Test data were reduced to frosting and defrosting loss coefficients and incorporated in a seasonal performance computer code developed at Oak Ridge National Laboratory. The code was then used to evaluate on a seasonal basis the magnitude of frosting and defrosting losses for demand and time-temperature defrost controls.

---

W. A. Miller, P.E., is a research engineer for the Efficiency and Renewables Section of the Energy Division of Oak Ridge National Laboratory.

## LABORATORY FACILITY

### The Test Heat Pump

The refrigerant circuit of the test heat pump is similar to conventional design, except for a manufacturer-installed liquid line-suction line heat exchanger, which is active only during heating mode operation. This heat exchanger heats refrigerant just before it enters the compressor. Liquid refrigerant is throttled by capillary tubes during both cooling and heating modes of operation. Both indoor and outdoor heat exchangers are of tube-and-plate-fin construction. The indoor heat exchanger is an A-frame coil having a distributor that evenly meters refrigerant between each side of the coil. The outdoor coil has 14 fins per inch, each fin being wavy or patterned with two complete waves per row. The coil also has three tube rows and is installed at roughly a 30° slant. The heat pump has a suction line accumulator. Sight glasses were installed in the accumulator and compressor housing for visual observations of refrigerant distribution during defrost operation.

Modifications were made to the electrical circuit of the heat pump for separate measurements of power supplied to the indoor blower motor, the outdoor fan motor, and the compressor motor. The indoor blower motor and compressor are two-pole, three-phase,\* three-wire induction motors having Y-connected stator windings. Power was supplied to these motors by an independent power source having a constant 60-Hz, 220-V ac, three-phase sinusoidal waveform. The single-phase, two-speed outdoor fan motor was operated at high speed during all testing.

### Test Stand

The split-system heat pump used in the study was installed in two separate environmental chambers capable of controlling both the dry-bulb and dew-point temperature. A host computer and a data acquisition system (DAS) monitored all temperatures, pressures, powers, and flows. The DAS provided random access sampling at rates of up to 200 samples per second under complete program control of the computer.

Heat exchanger wall temperatures and refrigerant circuit temperatures were monitored using thermal ribbon platinum resistance temperature detectors (RTDs). Refrigerant pressures were measured using bellows-actuated force balance transducers. The power consumption of the outdoor fan, indoor blower, and compressor was measured separately using watt transducers. Moisture content of conditioned air in the environmental chambers was measured using dew point hygrometers that measure the true dew-point temperature.

The air-side indoor and outdoor heat exchanger capacities were measured using thermopile grids, made of 24 American-wire-gage copper constantan wire, and ducted multipoint Pitot tube averaging traverses. A booster fan, driven by a variable-speed motor, was placed in series with the fan of the outdoor unit and was automatically controlled by the DAS and host computer to maintain a zero static pressure drop across the outdoor unit; thus the fan simulated free-flow conditions during the frosting test interval.

Single-phase refrigerant flow rate was measured in the liquid line using a turbine volume flowmeter.

## EXPERIMENTAL PROCEDURE

### Steady-State Tests

The heat pump operated inside the environmental chambers at controlled ambient temperature and humidity conditions. Temperatures and pressures in the refrigerant circuit, power consumption, and capacity were monitored for observation of established steady-state operation. On command, the DAS and host computer then monitored refrigerant-side and air-side data at 10-second intervals over a period of 0.5 h for use in calculating average COP and capacity. Calculated values of heating mode COP and capacity based on air-side measurements were within 3% of calculated values based on refrigerant-side measurements.

\*The inverters originally used with these motors were bypassed for these tests.

## Frosting-Defrosting Tests

Frosting-defrosting tests were performed to observe the effect of relative humidity and outdoor temperature on COP and capacity. These tests were conducted at outdoor air temperatures of 40 F, 35 F, and 25 F (4.4°C, 1.6°C, and -3.8°C) with outdoor relative humidities of 60%, 70%, and 80% per outdoor air temperature. The control of the heat pump and data collection were performed automatically by the data acquisition and host computer systems. Prior to actual data collection, the heat pump was run through a preliminary frosting and defrosting cycle at the desired ambient air test conditions. This was done to better simulate actual frosting and defrosting operation.

The defrosting cycle was initiated following the frosting interval using differing defrosting logics to compare their performance. A demand defrosting logic, based on a total air pressure drop of 0.51 inches (0.13 kPa) of water through the outdoor coil was used to start the defrost cycle on command by the DAS. The signals from the manufacturer-supplied demand sensor and from a differential pressure cell, which measured air-pressure drop, were both used as input to the DAS for start of defrost. Time-temperature logics, based on 90- and 45-minute timed cycles and entering evaporator temperature, were also tested for comparison of frosting and defrosting losses. Following the defrost cycle, the heat pump was returned to heating-mode operation, and the recovery time required to achieve 95% of steady-state capacity was recorded as well as refrigerant temperatures and pressures.

Frosting data were monitored at preset time intervals into the frosting, defrosting, and recovery cycles. As time progressed into the frosting and defrosting cycles, the scan rate was automatically adjusted according to the severity of the time-dependent transients. Upon completion of the test, data were recorded and filed on the host computer for further reduction and analysis.

## STEADY-STATE EFFICIENCY

The heat pump tested in these experiments yielded heating- and cooling-mode performance data that agreed well with the rated values published by the Air-Conditioning and Refrigeration Institute (ARI). The ARI ratings and observed values of COP and capacity of the test heat pump are listed in Table 1.

## EFFICIENCY UNDER FROSTING CONDITIONS AS A FUNCTION OF OUTDOOR TEMPERATURE

The efficiency of the test heat pump was only slightly affected by frosting of the outdoor coil for tests conducted at outdoor temperatures of 40 F, 35 F, and 25 F (4.4°C, 1.7°C, and -3.9°C) with the outdoor relative humidity held constant at 80%. Both the COP (Figure 1) and heating capacity showed only slight degradation despite coil frosting, which induced demand defrosting for tests conducted below 40 F (4.4°C) outdoor temperature. However, for the test conducted at 40 F (4.4°C) and 80% relative humidity, the heat pump operated for 7 hours with no frosting visually observed on the outdoor coil. Apparently mass transfer increased coil wall temperature above the freezing point of water, and therefore no frosting was observed on the coil.

## EFFICIENCY UNDER FROSTING CONDITIONS AT VARIOUS HUMIDITY LEVELS

Frosting tests conducted at 35 F (1.7°C) revealed slight degradation in COP and heating capacity for outdoor relative humidity ranging from 60% to 80%. The plots of COP and capacity shown in Figures 2 and 3, respectively, reveal only marginal drops in efficiency over time despite the accumulation of frost on the outdoor heat exchanger. However, the duration of each frosting test decreased due to the accumulation of frost on the outdoor coil. Each defrost cycle was initiated on demand once the total air-pressure drop through the outdoor coil exceeded 0.51 in (0.13 kPa) of water. The increase of air-pressure drop across the outdoor coil in Figure 4 gives an indication of the rate of frost accumulation on the outdoor coil. At an outdoor ambient condition of 35 F (1.7°C) and 60% relative humidity, the airflow dropped from 2500 to 1800 cfm (1180 to 850 L/s) in roughly 3.2 hours of frosting operation. Similar drops in outdoor airflow took 2 hours for the frosting test conducted at 70% outdoor relative humidity and only 75 minutes for the test conducted at 80% outdoor relative humidity. Thus, at the start of each defrost cycle, the outdoor coil was heavily laden with frost with

only slight free-flow area through the coil. However, despite these frost accumulations, the outdoor heat exchanger capacity decreased only marginally. As a result, the density of refrigerant entering the compressor remained fairly constant over time for all tests. These trends in turn caused the refrigerant mass flow rate and compressor power to be only slightly affected by frosting of the outdoor coil.

## OUTDOOR FAN CHARACTERISTICS OBSERVED UNDER FROSTING CONDITIONS

The characteristic curves for the outdoor fan are plotted in Figure 5 as a function of outdoor airflow. Results observed under the ambient conditions of 35 F (1.7°C) and 70% relative humidity reveal that the fan operated through a region of unstable performance from roughly 50 to 100 minutes of heat pump frosting operation. This region of unstable performance, seen by the slight dip in total air-pressure drop through the outdoor coil, is characteristic of all propellor fans and is caused by stalling\* of some part of the fan blades. This results in an instability and oscillation of air pressure, which is termed "surging" (Huppert 1951).

Frosting increased the resistance to airflow through the outdoor coil, and that in turn caused a change of operating point for the fan and coil combination. After 90 minutes, the airflow was reduced by 15% of its free-flow airflow of 2500 cfm (1180 L/s). Outdoor fan power dropped slightly from 45 minutes to 90 minutes due to the fan operating through its surge and stall region; however, as frosting continued and outdoor coil pressure drop increased, the outdoor fan power increased, as seen in Figure 5. The combination fan and fan motor mechanical efficiency dropped from 34.5% at near free-flow delivery to 33% after 100 minutes of coil frosting. At termination of the frosting test, the coil was visually observed to be heavily frosted with the majority of frost on the lower windward portion of the coil. The frost was fluffy, indicating a porous structure through which air could still pass across the coil.

Stalling of the fan blades had little effect on the total efficiency of the outdoor fan. However, the results suggest that the outdoor fan of a heat pump should be selected to operate through a range of air pressure drops that are below pressure drops in the region of fan stalling. This would result in maximum fan efficiency and reduced noise level and would cause less reduction in outdoor airflow, thereby prolonging time between defrosts.

## REVERSE CYCLE DEFROSTING

Capacity and compressor power trends are depicted in Figure 6 for a frosting-defrosting test conducted at an outdoor air temperature of 35 F (1.7°C) with 70% relative humidity. The reverse-cycle defrosting causes a chilling of the indoor return air, which must be tempered to maintain comfort conditions in the residence. The power draw of both the compressor and the auxiliary heaters during defrosting will increase the energy consumption and degrade efficiency.

The operation of the reverse-cycle defrost is next analyzed for better understanding of the effects of defrosting on heat pump components.

### The Dynamics of Heat Pump Defrosting

At the start of the defrost cycle, the four-way reversing valve is energized for cooling-mode operation and the outdoor fan is deenergized. The indoor coil, previously the condenser, holds approximately 50% of the total charge of 7.5 lb (3.4 kg), with the remainder of the charge distributed between the accumulator and the outdoor coil.† The heating capacity drops to near zero after only 30 seconds of defrosting (Figure 6) due to the redirection of hot superheated refrigerant from the compressor to the outdoor coil. The slave valve within the reversing valve energizes instantly at the start of defrost; however, the pressures measured across the indoor capillary tube indicate a negligible flow of refrigerant through the throttle for 1.5 minutes (Figure 7). Also the indoor coil pressure drops from 200 to 25 psia (138 to 173 kPa) as the compressor pumps refrigerant from the indoor coil for use in reverse-cycle defrosting.

\*Separation of flow occurs over a large part of the blade, resulting in disordered flow and a loss of lift and an increase of drag.

†This charge distribution is assumed from previous steady-state refrigerant weight measurements.

After only 30 seconds of defrosting, the refrigerant, having been pumped from the indoor coil, is now temporarily held in the accumulator, while the indoor coil holds primarily low-pressure vapor. With the indoor coil starved for refrigerant, the compressor power drops during the first 1.5 minutes of defrosting. Now, as in the situation observed during dry-coil cycling (Mulroy 1985), the refrigerant must be pumped through the small metering hole at the bottom of the U-tube within the accumulator. The increase in temperature difference between the accumulator wall\* (measured 3 inches from the bottom of the accumulator) and the saturated temperature of refrigerant at compressor inlet (plotted along with indoor coil capacity in Figure 8) indicates the movement of refrigerant from the accumulator. Little defrosting is accomplished during the first 1.5 minutes due to the temporary storage of refrigerant in the accumulator. Yet visually made observations through sight glasses indicate that the amount of refrigerant liquid entering the compressor is small because of the protection provided by the accumulator.

Outdoor coil refrigerant pressure begins to increase after 2 minutes of defrosting as refrigerant is pumped from the accumulator and made active within the refrigerant circuit. The majority of refrigerant is now in the outdoor coil, it being the condenser during defrost. Refrigerant temperature at exit of the outdoor coil, the signal used for defrost termination, remains fairly constant through 4 minutes of defrosting (Figure 9). Subcooling of refrigerant leaving the outdoor coil increases after the 2 minutes of initial defrost transients. The pressure drop across the indoor throttle also begins to increase, resulting in an increase of refrigerant mass flow toward the indoor coil and back to the accumulator and compressor. The return of two-phase refrigerant back to the accumulator decreases the difference between the accumulator wall temperature and the suction saturation temperature as the accumulator wall is cooled by the entering saturated refrigerant. The accumulator begins to fill again with refrigerant. The refrigerant suction pressure begins to increase as does refrigerant density entering the compressor. These increases in turn increase the compressor power draw from 2 minutes into defrosting until defrost termination.

As time progresses from 4 minutes to 6 minutes into defrosting, an increase can be seen in refrigerant pressure, temperature, and subcooling exiting the outdoor coil (Figure 9). However, after 6 minutes, the subcooling at the exit of the outdoor coil begins to drop, indicating that the subcooled region in the outdoor coil is decreasing as defrosting nears completion. The instantaneous capacity nears 2.5 tons (7.3 kW) cooling and requires a minimum of 4 kW of auxiliary heat from 2 minutes into defrost until defrost termination to negate the chilling of the indoor return air. The frost on the outdoor coil after 6 minutes of defrosting has now either melted or fallen off the coil, and as a result outdoor coil temperature and pressure continue to increase. Once the refrigerant temperature at the outdoor coil exit exceeds 75 F (24°C), defrost is terminated. For the above discussed test, defrosting is stopped after 7 minutes, as seen in Figure 9 by the increase in temperature at the exit of the outdoor coil. At this point in defrost time, only a 2-inch (50.8-mm) level of refrigerant can be visually observed in the accumulator. Also due to the declining subcooling and increasing temperature in the outdoor coil, the indoor coil probably holds the greater portion of refrigerant at the termination of defrosting.

## SEASONAL PERFORMANCE ANALYSIS

Seasonal analyses using the experimental data were conducted using a seasonal performance computer model† developed at Oak Ridge National Laboratory. The computer model is publicly available in Fortran IV language and can be run on a personal computer with nominally 120K of memory.

The experimentally observed average COP and capacity, integrated over the frosting and recovery intervals, were used to develop frosting loss coefficients that express the percentage loss in cumulative steady-state capacity and COP. Defrosting loss coefficients were also developed in a similar manner for expressing capacity and COP losses during defrost. The frosting and defrosting loss coefficients, frosting time, and defrost time were incorporated in the seasonal performance computer code as functions of outdoor ambient temperature, relative humidity, and style of defrost control. Algorithms developed from the frosting and defrosting data were coupled to a quadratic interpolation routine for use in calculating the breakdown of annual energy consumption due to frosting and defrosting for the various defrost controls.

Although not specifically addressed in this report, cycling and off-cycle parasitic (40-W crankcase heater) losses are included in the seasonal analyses. Cooling and heating mode cycling tests were conducted with nameplate charge in the heat pump according to the Department of Energy (DOE) test procedures (1979). Measured cyclic COP ratios as function of load factor were then used for the seasonal analysis calculation of cycling losses.

\*This represents refrigerant saturated temperature in accumulator.

†The computer code was developed by Rice, Fischer, and Emmerson (1986).

Seasonal performance simulations were conducted for the test heat pump operating in Fort Worth, TX; Knoxville, TN; and Syracuse, NY, in "standard houses." The standard house used for the analysis is a ranch-style single-family detached residence with 1800 ft<sup>2</sup> (167 m<sup>2</sup>) of living area and a crawl space. The house is oriented in an east-west direction and has one air change per hour at 15-mph (24.2-km/h) outdoor wind speed and 70 F (39°C) inside-outside temperature difference. Single-glazed windows cover a nominal 15% of the exterior surface area. The ceilings are insulated to an R-19 level, the walls to an R-11 level, and the floors to an R-9 level. With the above-described standard house as a basis, the heating and cooling loads were calculated per seasonal analysis for each of the cities using a weather data base obtained from the U.S. Air Force manual on engineering weather data (1978).

## ENERGY CONSUMPTION FOR DIFFERENT DEFROST CONTROLS

The predicted dynamic loss energy consumptions are listed in Table 2 for the test heat pump operating with demand- and time-temperature defrost controls in the standard houses in Fort Worth, TX; Knoxville, TN; and Syracuse, NY, respectively. These cities are representative of the range of climates throughout the United States.

For Fort Worth, the test heat pump is nominally 14% oversized, having a 1.14 cooling design factor (CDF), which is the ratio of cooling load to steady-state cooling capacity at the 97.5% ASHRAE design day temperature. The frosting-defrosting losses are 1.1% of total annual energy, and backup resistance heat is only 0.9% of the total heat pump annual energy consumption for demand defrost simulation. The small losses due to frosting, defrosting, and backup heat are the results of the yearly load being predominantly cooling, as seen by the ratio of heating load to yearly load in Table 2.

The seasonal analysis for Knoxville showed frosting losses to be only 2.0% to 3.6% of total energy usage. The defrost losses increased as the defrost control was changed from demand defrost control to a 45-minute time-temperature defrost control. Demand defrosting contributed to 1.5% of the total annual energy, and the time-temperature defrosting using 90- and 45-minute timed cycles contributed to 5.1% and 8.5%, respectively, of total annual energy. Predicted yearly defrosts increased from 303 defrosts per demand control to 911 and 2013 defrosts, respectively, for 90-minute and 45-minute timed cycle controls (Table 2).

In the more severe winter climate of Syracuse, the relationship of frosting-defrosting losses and backup heat energies changes dramatically as compared with Fort Worth and Knoxville. The frosting and demand defrosting losses, being 6.5% of total yearly energy, are greater than those observed for Fort Worth or Knoxville. Frosting of the outdoor coil accounted for nominally 3.6% of the total yearly energy consumed. Demand defrosting accounted for 2.8% of the total energy, and backup heat accounted for 19.9%. Due to the large heating load, the energy use of backup resistance heat was greater than the frost-demand defrost loss energy. However, this trend changes for time-temperature control (Table 2). There were 816 predicted yearly demand defrosts; for 90- and 45-minute timed-defrost cycles, yearly defrosts increased dramatically to 2008 and 4348 occurrences, respectively.

The seasonal analysis results quantify the benefits of the demand defrost control in terms of total energy use and therefore in terms of annual performance factor (APF). As seen in Table 2, the difference in defrost losses for demand defrosting and 90-minute time-temperature defrosting for the three cities is roughly 2% to 6% of total heat pump energy. The frosting-defrosting tests showed that the 90- and 45-minute cycles allow defrosting operations too frequently for most ambient conditions less than 40 F (4.4°C) with relative humidities greater than 70%. Increasing the time period would alleviate this problem; however, under severe outdoor ambient temperatures with relative humidities greater than 90%, the longer timed-defrost cycle may not maintain system reliability.

The seasonal analysis clearly shows that frequent defrosting causes the frosting-defrosting degradation to be due primarily to defrosting of the outdoor heat exchanger. Results indicate that the demand-defrost control yields best seasonal efficiency while maintaining system reliability under severe frosting conditions for locations such as Syracuse.

## HEAT PUMP ANNUAL OPERATING COSTS

The frosting and defrosting portions of annual consumed energy can be translated into direct costs to determine incremental paybacks for improving heat pump efficiency. Energy costs based on electric rates taken from the DOE publication *Typical Electric Bills* (1985), were used to calculate annual operating costs. The electric rates, which were based on summer and winter costs per 1000 kWh, were used to calculate cost data shown in Table 3 from the energy consumption listed in Table 2.

For Fort Worth and Knoxville, which have a ratio of heating load to total load of less than 0.6, the cost of consumed energy for backup heat was only \$10.00 or less per year. In contrast, for Syracuse, which has a heating to total load ratio greater than 0.6, heat pump operating costs increased significantly. The cost of backup heat increased to about \$208 per year.

Total heat pump operating cost is greatest for Syracuse, because of the required use of backup heat and high utility rates. The cost of energy losses due to frosting and demand defrosting are \$68 for Syracuse and \$16 or less for Knoxville and Fort Worth. Knoxville's lowest yearly operating cost is due simply to lower utility rates (Table 3).

Three-year potential paybacks shown in Table 4 are based on the assumption that the test heat pump operates with a demand-defrost control as compared with a 90-minute and also a 45-minute time-temperature defrost control. For Fort Worth, which has predominantly a cooling load, the use of a demand defrost control yielded marginal cost savings as compared with the 90-minute time-temperature defrost control. In predominately heating load climates, paybacks are more attractive. With a 3-year payback, the consumer could afford the amounts listed in Table 4 for the respective cities for improved defrost hardware. Although payback for improved defrost control is not favorable for all U.S. cities investigated, the use of the demand defrost control yielded best seasonal performance across the country. An extension of the demand-defrost interval for heat pump operation in Syracuse would further improve payback potential to the consumer in New York. Because frosting losses are minimal, defrost intervals can be extended provided system reliability is not compromised. Further research would be required to develop best defrost frequency in terms of cost savings, annual efficiency, and system reliability.

## SEASONAL ANALYSIS FOR A HYPOTHETICALLY SIZED HEAT PUMP

All seasonal analyses discussed so far were conducted by simply applying the 2 3/4-ton (9.7-kW) test heat pump to weather data for the various cities. The ASHRAE design procedures (ASHRAE 1983) imply that the heat pump should be sized to the design cooling load calculated at a design temperature that is greater than observed daily temperatures 97.5% of the time. However, such sizing criteria do not always yield the best APF for a given design of heat pump.

So that the effect of oversizing on APF could be observed, (1) steady-state capacities and power consumptions (both heating and cooling), (2) frosting, defrosting, and cycling capacities, and (3) power consumption measured for the test heat pump (operating with demand defrost) were scaled to yield various degrees of oversizing. It was assumed that the frosting and defrosting time intervals would be independent of size (i.e., coil loading constant with scaling).

The plots of APF as a function of degree of heat pump oversizing (Figure 10) show that the 2 3/4-ton (9.7-kW) test heat pump yields near the best APF. For Fort Worth, sizing the heat pump to the design cooling load resulted in an APF of 2.13; for the 2 3/4-ton (9.7-kW) test unit, the calculated APF was 2.11. In Knoxville, the hypothetical unit sized to the design cooling load resulted in an APF of 2.01; for the 2 3/4-ton (9.7-kW) test unit, the APF was 2.00. As seen in Figure 10, oversizing the test heat pump for these two cities caused a reduction of APF because the oversized heat pump cycles more frequently, causing an increase in total annual energy consumption.

The trends of APF as a function of size for Syracuse differ from those for Knoxville and Fort Worth. In Syracuse, due to the higher heating load, increasing the size of the heat pump resulted in a decrease in the energy consumed by backup heat, although cycling losses do increase some. For the hypothetical heat pump sized to twice the cooling load in Syracuse, the energy consumed by backup heat decreased by 4200 kWh per year compared with the backup heat energy draw required for a heat pump sized to design cooling load. Cycling energy consumption increased; however, total annual operating energy decreased. These trends result in an increase in APF as size increases. The improvement in APF for Syracuse began to level off for sizes greater than twice the design cooling load. It should be noted here that the best APF for Syracuse may not be acceptable in terms of cost premium for oversizing or in terms of summer comfort conditions. The frequent cycling of the oversized unit would not allow proper control of humidity in the residence during the summer months. Further research on summer indoor humidity control would help establish proper heat pump sizing limits for northern climates.

## CONCLUSIONS

1. The accumulation of frost on the tube-and-plate-fin outdoor heat exchanger with 14 fins per inch had marginal effect on evaporator load, which in turn caused only 1% to 5% degradations in COP and capacity.

2. The test heat pump operating with a demand-defrost control yielded better seasonal efficiency than the 90- and 45-minute time-temperature controls for the various U.S. cities investigated through seasonal analysis.
3. Reverse-cycle defrosting was the predominant loss as compared with the frosting loss for time-temperature defrost control. However, demand defrosting was roughly 3% or less of annual heat pump energy consumption, and frosting of the outdoor coil accounted for roughly 2.5% of heat pump energy usage.
4. In northern climatic applications, the consumer can save roughly \$200 to \$400 over 3 years using demand-defrost hardware as compared with conventional 90- and 45-minute time-temperature defrost hardware.
5. Climates in which the cooling load was predominant had only marginal cost savings for demand-defrost controls; however, results indicate that the demand interval could be extended to maximize seasonal performance and still probably provide system reliability.
6. Qualitative analysis of the defrosting cycle indicates that the surging of refrigerant into the accumulator at start of defrost delays the completion of the defrosting cycle, which in turn degrades seasonal efficiency.
7. For the locations studied, oversizing above the design cooling load was of minimal benefit except for the northernmost climates, where oversizing was beneficial subject to oversizing cost premium and uncertain limits on oversizing to maintain humidity control.
8. The outdoor propeller fan of a heat pump should be designed to operate during outdoor coil frosting through a range of pressure drops that are below pressure drops in the operating region of fan-blade stalling.

## REFERENCES

- ASHRAE. 1983. *ASHRAE Handbook—1983 Equipment*. "Unitary heat pumps and packaged terminal heat pumps: equipment design and selection," Atlanta: American Society of Heating, Refrigerating, and Air-Conditioning Engineers, Inc., pp. 44.4.
- Department of Energy. 1979. "Test procedures for central air conditioners, including heat pumps." 10CFR Part 430, *Federal Register*, Vol. 44, No. 249, pp. 76700-76723.
- Department of Energy. 1985. "Typical electric bills," DOE/EIA-0040(85).
- Departments of the Air Force, Army, and Navy. 1978. "Engineering weather data," documents AFM 88-29 (Air Force), TM5-785 (Army), and NAVFAC P-89 (Navy).
- Huppert, M. C., and Benser, W. A. 1951. "Some stall and surge phenomena in axial flow compressors." Vol. 73, p. 835.
- Miller, W. A. 1982. "Laboratory evaluation of the heating capacity and efficiency of a high-efficiency, air-to-air heat pump with emphasis on frosting/defrosting operation." ORNL/CON-69. Oak Ridge National Laboratory.
- Miller, W. A. 1984. "Frosting experiments for a heat pump having a one-row spine-fin outdoor coil." *ASHRAE Transactions*, Vol. 90, Part 1.
- Mulroy, W. J., and Didion, D. A. 1985. "Refrigerant migration in a split-unit air conditioner." *ASHRAE Transactions*, Vol 91, Part 1.

Research sponsored by the Office of Buildings and Community Systems, U.S. Department of Energy, under contract DE-AC05-84OR21400 with Martin Marietta Energy Systems, Inc.

**TABLE 1**  
**Observed Steady-State Performance Compared with**  
**Air-Conditioning and Refrigeration Institute Ratings**

Organization	Supply air [cfm (m <sup>3</sup> /s)]	Cooling mode		Heating mode <sup>b</sup>	
		Capacity [MBtu/h (kW)]	EER <sup>a</sup>	Capacity [MBtu/h (kW)]	COP
ARI rating	1275 (36)	34.0 (9.9)	7.4	38.0 (11.1)	3.0
ORNL data	1275 (36)	34.2 (10.0)	7.8	35.0 (10.3)	3.0

<sup>a</sup>Energy efficiency ratio.

<sup>b</sup>Outdoor dry-bulb temperature 47 F (8.3°C).

**TABLE 2**  
**Percentage of Total Annual Heat Pump Energy Consumption**

City, state	Defrost control <sup>a</sup>	Ratio of heating load to annual load	Annual backup heat use <sup>b</sup> (% of total)	Annual energy losses (% of total)		Yearly defrosts	Total annual energy <sup>d</sup> (kWh)
				Frosting <sup>c</sup>	Defrosting		
Fort Worth, TX	Demand	0.32	0.90	1.01	0.80	183	10566.0
	90 min		0.87	1.47	2.50	519	10822.0
	45 min		0.85	1.99	4.28	1150	11098.5
Knoxville, TN	Demand	0.58	2.51	2.06	1.54	303	9337.9
	90 min		2.40	2.81	5.05	911	9799.4
	45 min		2.28	3.64	8.51	2013	10299.7
Syracuse, NY	Demand	0.84	19.94	3.65	2.82	816	15411.9
	90 min		18.67	3.86	8.39	2008	16456.5
	45 min		17.39	4.18	14.00	4348	17668.2

<sup>a</sup>Demand defrost initiated by air-pressure drop across the outdoor coil. Time-temperature defrost initiated by specified time and liquid line temperature.

<sup>b</sup>Auxiliary heat required to satisfy house heating load when heat pump operates below balance point. Does not include auxiliary heat (5 kW) attributed to reverse-cycle defrost.

<sup>c</sup>Frosting includes recovery energy following defrost plus auxiliary heat consumed due to effect of frosting on heat pump balance point.

<sup>d</sup>Heat pump yearly energy consumption including back-up heat.

TABLE 3

## Annual Cost Breakdown of Energy Consumed by the Test Heat Pump

City, state	Defrost control <sup>a</sup>	Ratio of heating load to annual load	Annual backup heat cost <sup>b</sup> (\$)	Annual cost of dynamic energy losses <sup>c</sup> (\$)		Total energy cost <sup>c</sup> (\$)
				Frosting <sup>d</sup>	Defrosting	
Fort Worth, TX	Demand	0.32	6.02	6.81	5.26	750.02
	90 min			10.12	17.24	766.32
	45 min			14.08	30.26	788.92
Knoxville, TN	Demand	0.58	11.05	9.05	6.75	439.44
	90 min			12.95	23.29	461.16
	45 min			17.66	41.26	484.70
Syracuse, NY	Demand	0.84	208.45	38.16	29.52	1045.40
	90 min			43.14	93.64	1116.24
	45 min			50.15	167.85	1198.43

<sup>a</sup>Demand defrost initiated by air-pressure drop across the outdoor coil. Time-temperature defrost initiated by specified time and liquid line temperature.

<sup>b</sup>Auxiliary heat required to satisfy house heating load when heat pump operates below balance point. Does not include auxiliary heat (5 kW) attributed to defrost.

<sup>c</sup>Costs based on winter and summer electric rates.

<sup>d</sup>Frosting energy costs include recovery energy costs and auxiliary heat use due to effect of frosting on heat pump balance point.

TABLE 4

## Payback for Reduction of Frost-Defrost Losses with Demand vs. Time-Temperature Controls

City, state	Ratio of heating load to annual load <sup>a</sup>	Cost premium (\$) for 3-year payback	
		Demand vs. 90 min	Demand vs. 45 min
Fort Worth, TX	0.32	46.00	97.00
Knoxville, TN	0.58	61.00	130.00
Syracuse, NY	0.84	207.00	451.00

<sup>a</sup>Loads calculated using Air Force engineering weather data base applied to 1800-ft<sup>2</sup> (167-m<sup>2</sup>) ranch-style house with minimum insulation as specified by Housing and Urban Development.

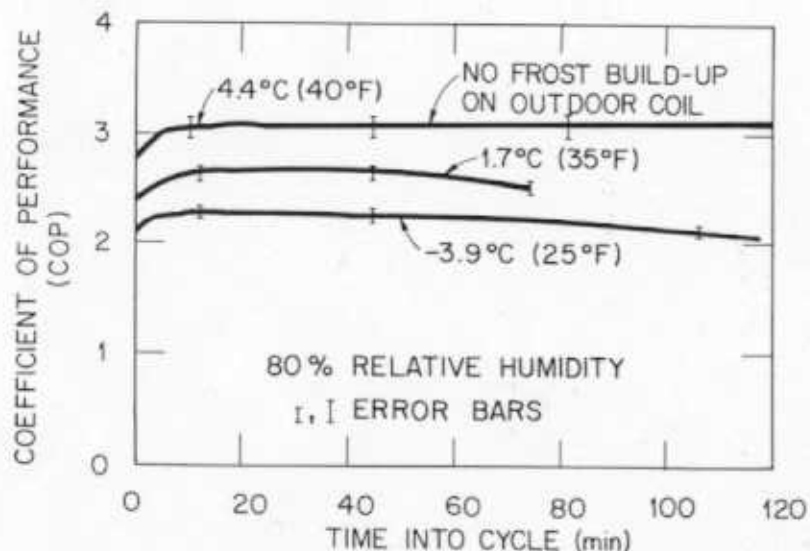


Figure 1. COP observed for various outdoor temperature frosting tests, each having 80% outdoor relative humidity

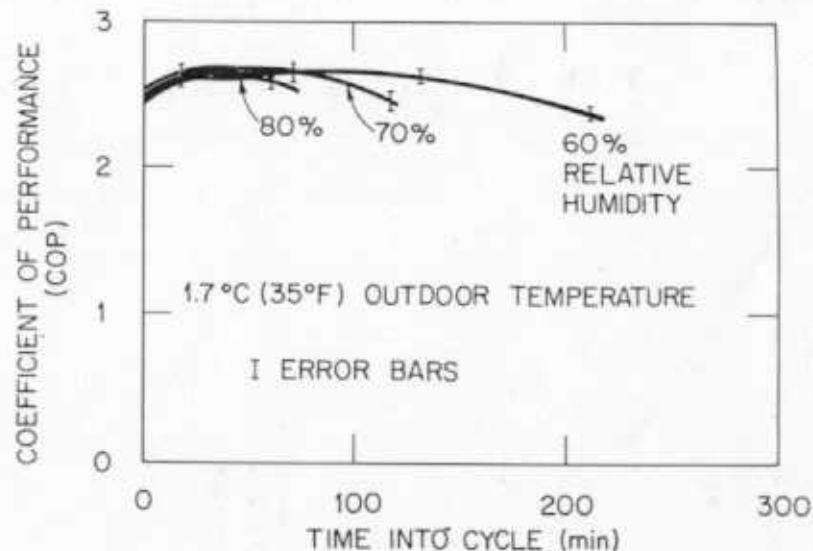


Figure 2. The COP observed for frosting tests conducted at an outdoor air temperature of 35 F (1.7°C)

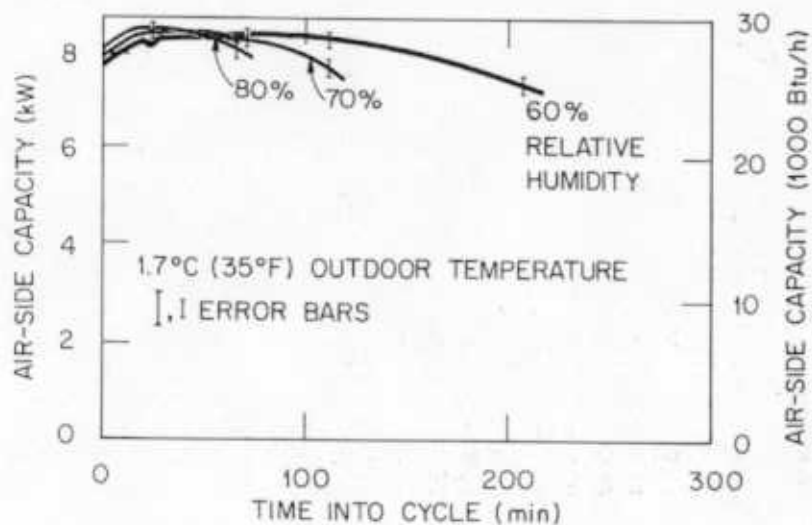


Figure 3. Air-side capacity measured during frosting tests conducted at 35 F (1.7°C) outdoor air temperature

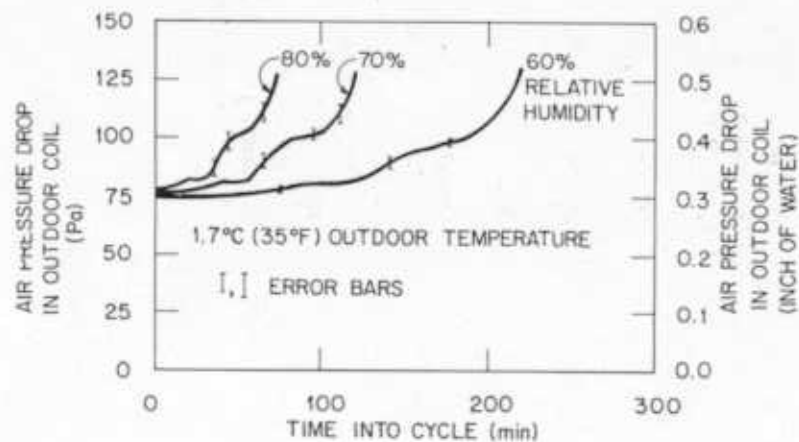


Figure 4. Air pressure drop measured across the outdoor coil under frosting conditions at 35 F (1.7°C) outdoor air temperature

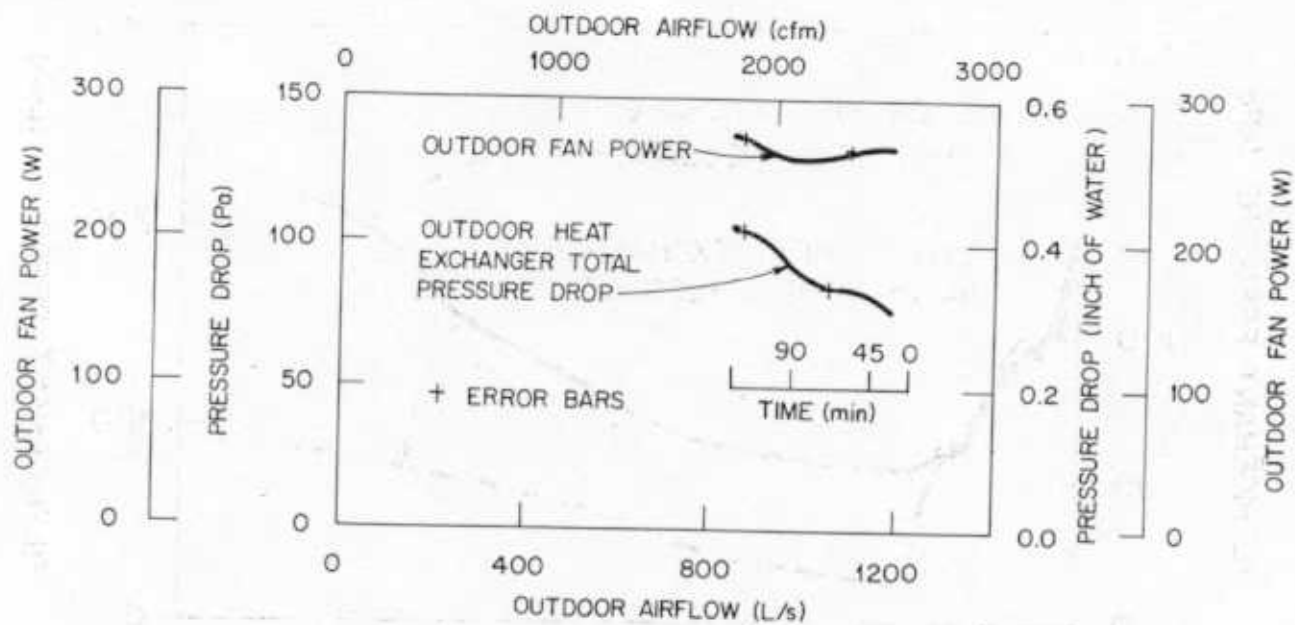


Figure 5. Outdoor propeller fan characteristics observed during frosting tests conducted at 35 F (1.7°C) outdoor temperature and 70% relative humidity

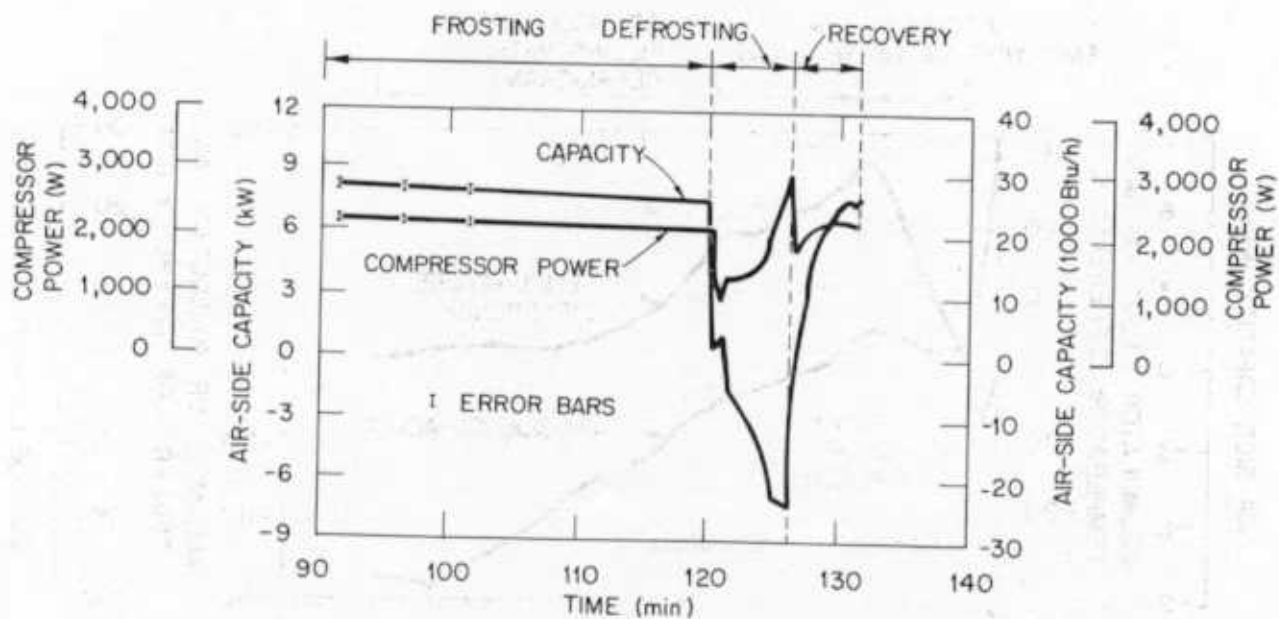


Figure 6. Frosting-defrosting-recovery test conducted at 35 F (1.7°C) outdoor air temperature and 70% relative humidity

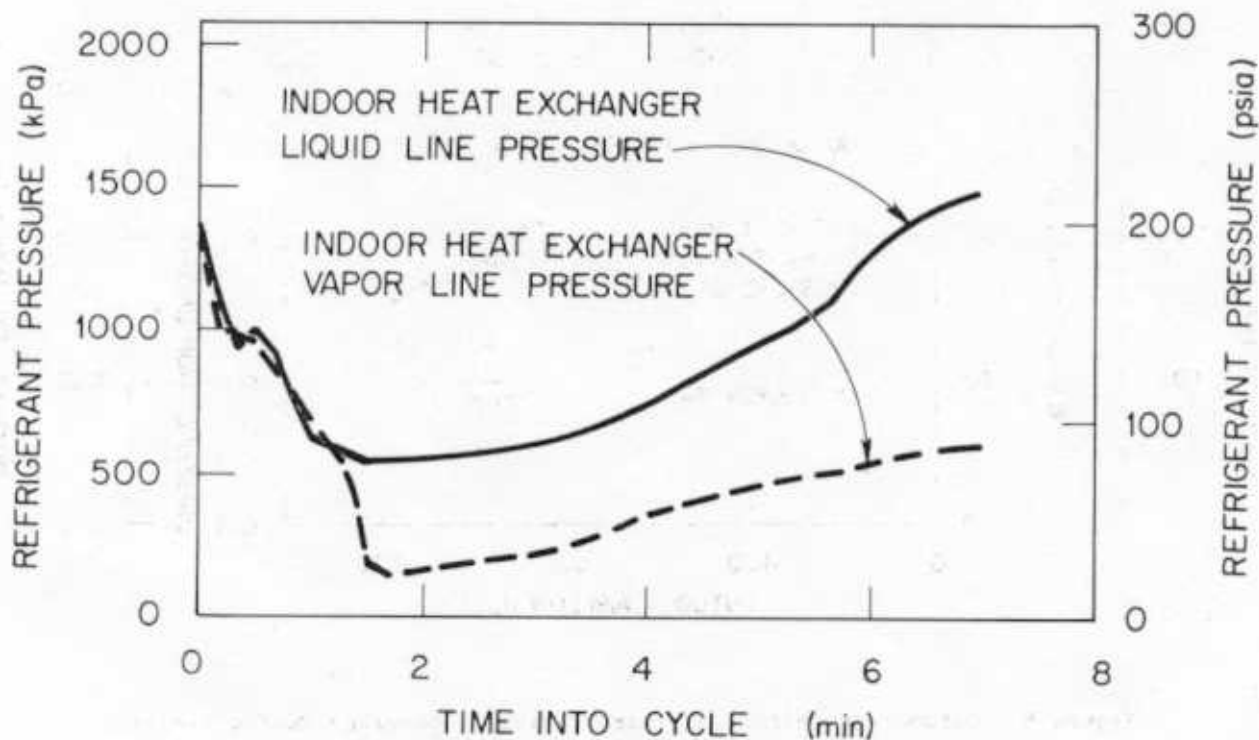


Figure 7. Refrigerant pressures measured across the indoor capillary tubes during defrost with 35 F (1.7°C) outdoor air temperature and 70% relative humidity

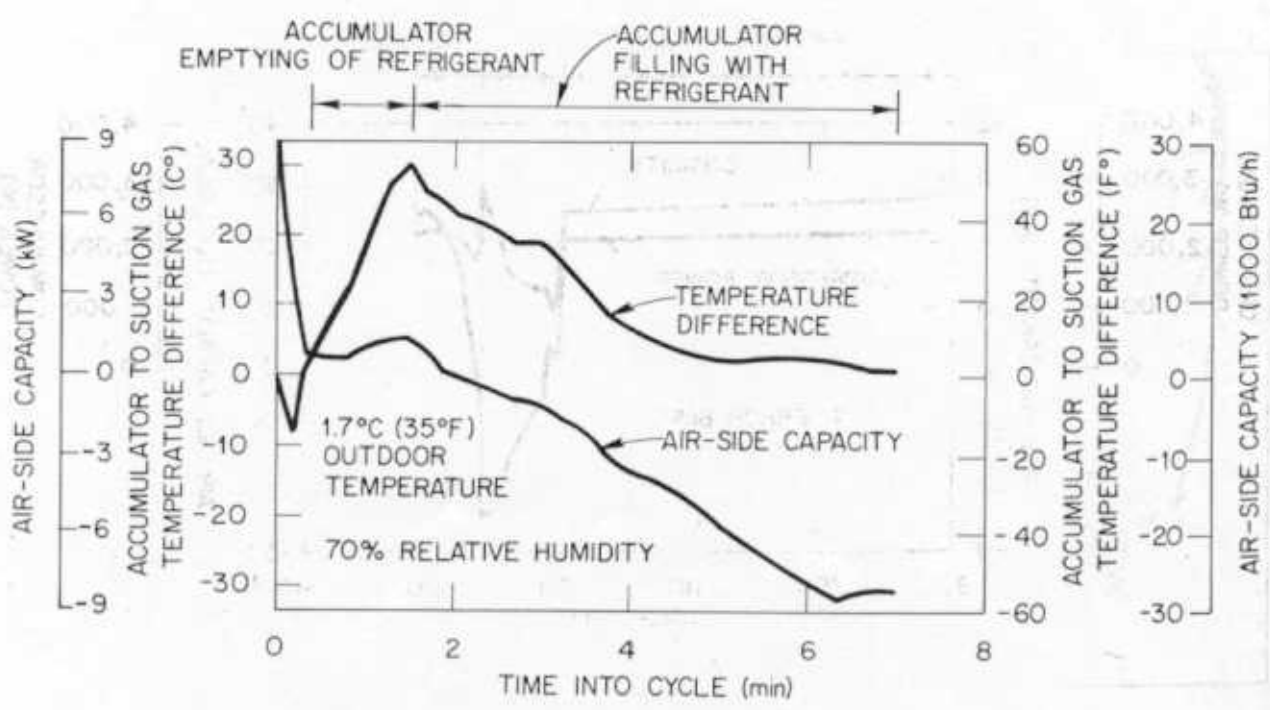


Figure 8. Air-side capacity during defrost as affected by the time required to pump refrigerant from the accumulator

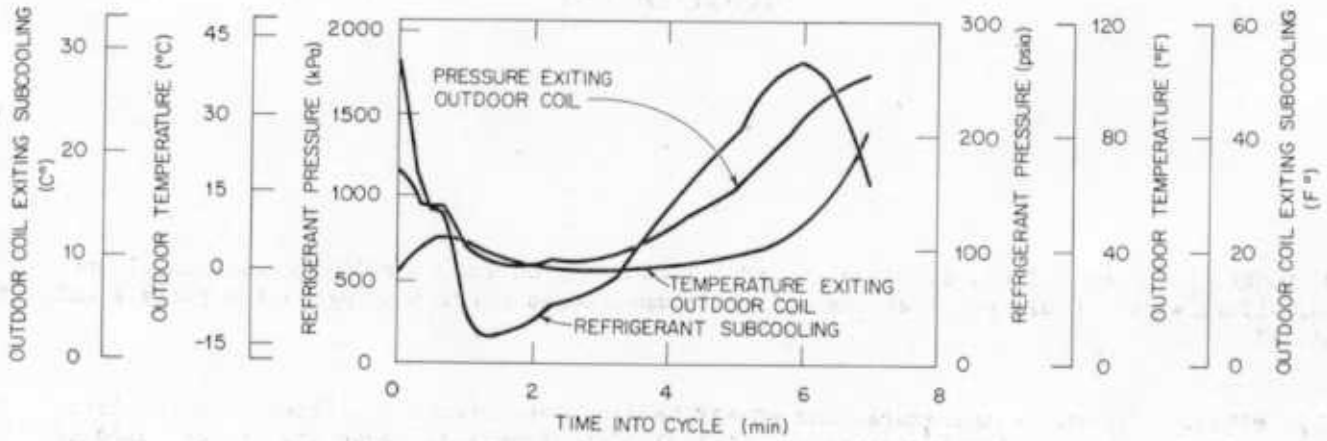


Figure 9. The state point of refrigerant exiting the outdoor coil during defrost conducted at 35 F (1.7°C) outdoor air temperature and 70% relative humidity

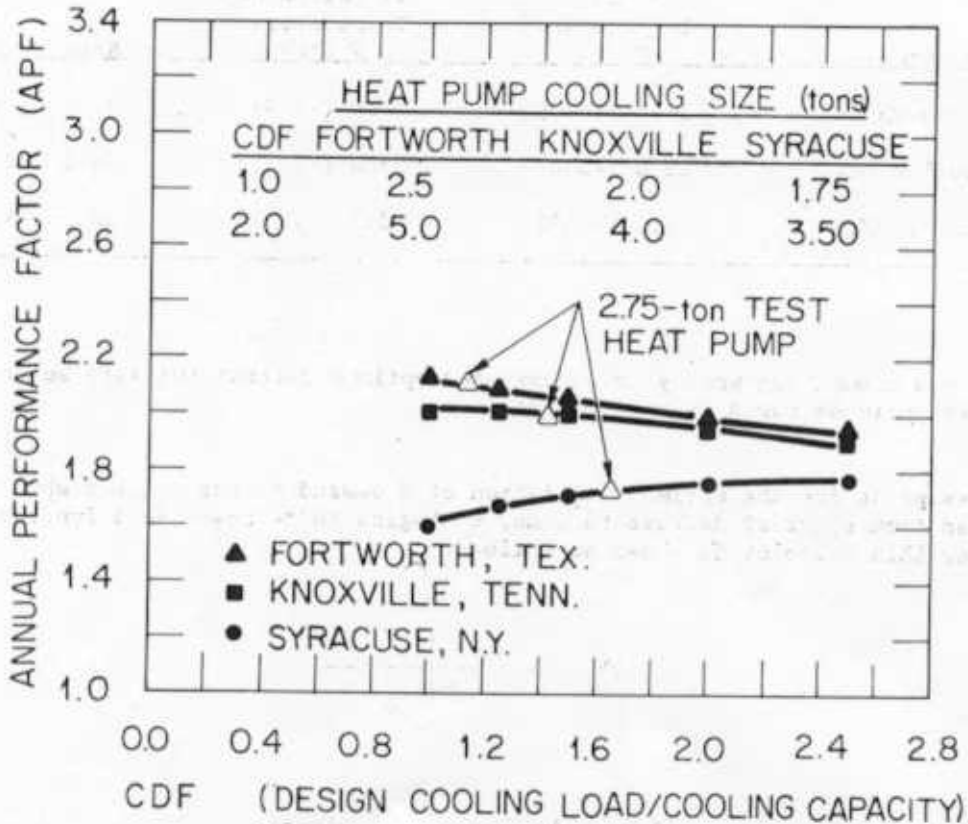


Figure 10. The annual performance factor as function of oversizing ratio

# Discussion

U. BONNE, Honeywell, Inc., Bloomington, MN: I commend you for your fine experimental and analytical work. Could you list the balance temperatures corresponding to the three simulated sites?

W.A. MILLER: Balance temperatures and ASHRAE heating load design conditions are tabulated below for the three cities investigated. Calculation of balance temperatures are based on seasonal performance simulations for the 2.75-ton (9.7-kW) heat pump operating in a ranch-style residence with 1800 ft<sup>2</sup> (167 m<sup>2</sup>) of living area (see text for further description).

City, State	Balance Temperature F (°C)	Heating Load Design Conditions	
		99% Design Day Temperature F (°C)	Design Load Kbtu/h (kW)
Fort Worth, TX	20.0 (-6.7)	17.8 (-7.9)	32.5 (9.5)
Knoxville, TN	22.0 (-5.6)	13.0 (-10.6)	35.8 (10.5)
Syracuse, NY	27.0 (-2.8)	-3.0 (-19.4)	48.5 (14.2)

BONNE: Could you comment on what your recommended optimum defrost-initiate setpoint (minimum operating cost) would be for a demand defrost?

MILLER: The setpoint for the optimal initiation of a demand defrost occurs when the average COP, integrated from start of defrost to time,  $t$ , begins to decrease as a function of time. Formulation for this setpoint is shown as follows:

$$COP_{avg} = \frac{\int_{ds}^t \dot{Q} dt}{\int_{ds}^t \dot{W} dt}$$

where

- Q = Instantaneous rate of heat delivered to residence,
- W = Total power draw of heating system,
- ds = Time coincident with start of defrost, and
- t = Time after defrost when COP<sub>avg</sub> decreases.

This optimal defrost interval would vary per heat pump due to differences in geometry, surface area, mass, and loading of the outdoor coil. Outdoor fan characteristics and horsepower rating of the outdoor fan motor cause differences in the optimal defrost interval per heat pump. Thus, in terms of a specific time interval, a definitive answer is not applicable; however, the above formulation of average COP initial decrease can be generalized to all air-to-air heat pump systems. For the unit tested in the laboratory, the setpoint of air pressure drop exceeding 0.51 in (0.13 kPa) of water appears close to the optimal demand defrost-initiate setpoint (review Table 2 of main text). Laboratory data suggest that the setpoint could be increased to 0.65 in (0.17 kPa) of water drop without affecting system reliability.

BONNE: Would the same setpoint hold true (at least approximately) as a function of balance point and refrigerant charge?

MILLER: The above formulation for demand defrost interval would be correct; however, both refrigerant charge and balance point affect the time of the optimal defrost interval. The loss of refrigerant charge decreases suction pressure and lowers the effective evaporating temperature. This, in turn, increases the rate of frost accumulation on the outdoor coil, thereby increasing defrost frequency. Oversizing the heat pump lowers the balance temperature and could possibly cause an increase loading of the outdoor coil depending on the relation of the outdoor coil size with sizing of the heat pump. Again, the rate of frost accumulation on the outdoor coil increases with a more fully loaded outdoor coil. However, a demand defrost sensor would properly adjust the defrost interval to compensate for any change of outdoor coil loading. Thus, defrost efficiency would be optimal for the given system, but it would not necessarily be the optimum due to loss of refrigerant charge or due to increased loading of the outdoor coil.